Dissolution, Transport, and Fate of Lead on Shooting Ranges

Caleb D. Scheetz

Thesis submitted to the faculty of the Virginia Polytechnic Institute and State University in partial fulfillment of the requirements for the degree of

Masters of Science

In

Geological Sciences

J. Donald Rimstidt, Chair

Madeline Schreiber

Lucian Zelazny

February 11, 2004

Blacksburg, VA

Keywords: Shooting range, lead, corrosion, soil, shot, hydrocerussite, cerusstie, and sequential extractions

DISSOLUTION, TRANSPORT, AND FATE OF LEAD ON SHOOTING RANGES

CALEB D. SCHEETZ

ABSTRACT

Shooting ranges concentrate significant quantities of heavy metals, especially lead as spent shot and bullets, on very small parcels of land. Samples taken from a shooting range near Blacksburg, VA, USA provide information about the reservoirs and pathways of lead at shooting ranges in an upland setting and humid environment. Metallic lead corrodes rapidly and develops a coating of corrosion products. The type and amount of corrosion products found on lead shot and bullets are best understood through examination of Eh-pH relationships. X-ray diffraction analysis identified hydrocerussite ($Pb_3(CO_3)_2(OH)_2$) as the corrosion phase present on lead shot recovered from the range. Hydrocerussite dissolution can produce soluble lead concentrations ranging from 2 ppb to 2 ppm for the soil pH values at this site. This soluble lead is captured by the soil. Sequential chemical extractions revealed that vertical lead migration beyond the A-horizon was minimal. The bound-to-Fe & Mn oxides and bound-to-carbonates soil fractions were identified as significant reservoirs for sequestration of lead in the soil. The highest concentration of extractable lead contained in the soil was directly correlated with the highest concentration of lead shot and bullets measured on the shotgun range surface. The geochemical framework for understanding the corrosion process, identifying the corrosion product(s) that control lead solubility, and identifying the geochemical barriers to lead migration that were employed at the Blacksburg, VA shotgun range, provides a basis for selecting best management practices for this and other shooting range.

TABLE OF CONTENTS

LIST OF FIGURES	iv
LIST OF TABLES	v
INTRODUCTION	1
MATERIALS AND METHODS	3
RESULTS	10
DISCUSSION	14
BEST MANAGEMENT PRACTICES	24
REFERENCES	27
APPENDIX 1	32
APPENDIX 2	33
APPENDIX 3	38
APPENDIX 4	44
APPENDIX 5	45
APPENDIX 6	47

LIST OF FIGURES

FIGURE 1. Pathways and reservoirs for lead on shooting ranges. 3

FIGURE 2. Blacksburg shotgun range location. 5

FIGURE 3. Soil Sample locations. 7

FIGURE 4. Geometric mean Pb concentrations. 12

FIGURE 5. Distribution of surface concentrations and extractable concentrations. 13

FIGURE 6. Hydrocerussite and Cerussite Solubility. 15

FIGURE 7. Eh-pH diagram. 17

FIGURE 8. SR-22 Extractable Pb concentrations. 26

LIST OF TABLES

TABLE 1. Average soil pH. 19

INTRODUCTION

Shooting ranges provide safe, controlled environments for the discharge of firearms by recreational shooters, as well as police and military personnel. The congregation of shooters at shooting ranges concentrates spent lead shot and bullets onto very small parcels of land. The EPA estimates that roughly 7.26 x 10^7 kg of lead shot and bullets enter the U.S. environment each year at roughly 9000 non-military outdoor shooting ranges (EPA 2001). An average shot contains up to 97% metallic lead, 2% antimony, 0.5% arsenic, 0.5% nickel and jacketed bullets contain up to 90% metallic lead, 9% copper, and 1% zinc (Tanskanen 1991). Corrosion of these materials could potentially release significant quantities of these metals into the environment.

Because of its toxicity, lead is of particular concern. Lead toxicity to humans and wildlife has been extensively documented. In humans, prolonged exposure to high concentrations of lead can lead to brain, nervous system and reproductive damage (Posner 1978). Children are at particular risk because their bodies absorb lead more efficiently, so exposure to even low concentrations of lead can be seriously damaging to a child's health (Rosen 1978). The effects of lead poisoning in waterfowl by ingestion of lead shot are well documented (Feierabend 1983; Sanderson 1986); as a consequence restrictions have been placed on the use of lead shot for water fowl hunting.

Lead accumulation rates on shotgun ranges have been reported as ranging from 1.4 metric tons per year (Craig 2002) to greater than 15 metric tons per year (Tanskanen 1991) depending on usage. Soil lead concentrations of greater than 1000 mg/kg were reported for shotgun ranges in Denmark, England, Finland, New Zealand, Sweden, Switzerland, and the United States (Jorgensen 1987; Tanskanen 1991; Mellor 1994; Lin

1995; Rooney 1999; Craig 2002; Knechtenhofer 2003). Lead metal rapidly oxidizes in shooting environments leading to the formation of lead carbonate, oxide, and sulfate corrosion products (Jorgensen 1987; Lin 1995; Lin 1996; Chen 2002; Cao 2003). Murray (1997) reported that lead contamination from a shooting range in Michigan could potentially impact the local groundwater. Bruell (1999) reported that a shooting range with lead contaminated soil leached enough lead to pose a significant risk to associated surface and groundwater. Several authors have reported limited vertical lead migration in shooting range soils beyond the surface horizon (Lin 1995; Astrup 1999; Chen 2001; Chen 2002). Several previous studies have utilized the toxicity characteristic leaching procedure (TCLP) on shooting ranges (Pott 1993; Murray 1997; Bruell 1999; Basunia 2001; Chen 2001; Chen 2002; Cao 2003) to determine the potential hazard that the lead might pose to the groundwater system and if the soil should be considered hazardous waste. However, the TCLP was designed to model municipal solid waste landfill effluent. So it may not be the best method to identify reservoirs and pathways for lead on shooting ranges. A more suitable method to ascertain the potential mobility of lead on shooting ranges would be through the use of selective sequential extractions. Selective sequential extractions, furnish detailed information about the mode of occurrence, biological and physicochemical availability, and potential for mobilization and transport of trace metals (Tessier 1979).

The purpose of this paper is to provide a geochemical framework for understanding the corrosion process, identifying corrosion product(s) that control lead solubility, identifying geochemical barriers to lead migration, and integrating this knowledge into a set of best management practices for a shotgun range at a site in

southwestern Virginia. Figure1 is a conceptual model of the possible reservoirs and transport pathways for lead on a shooting range.

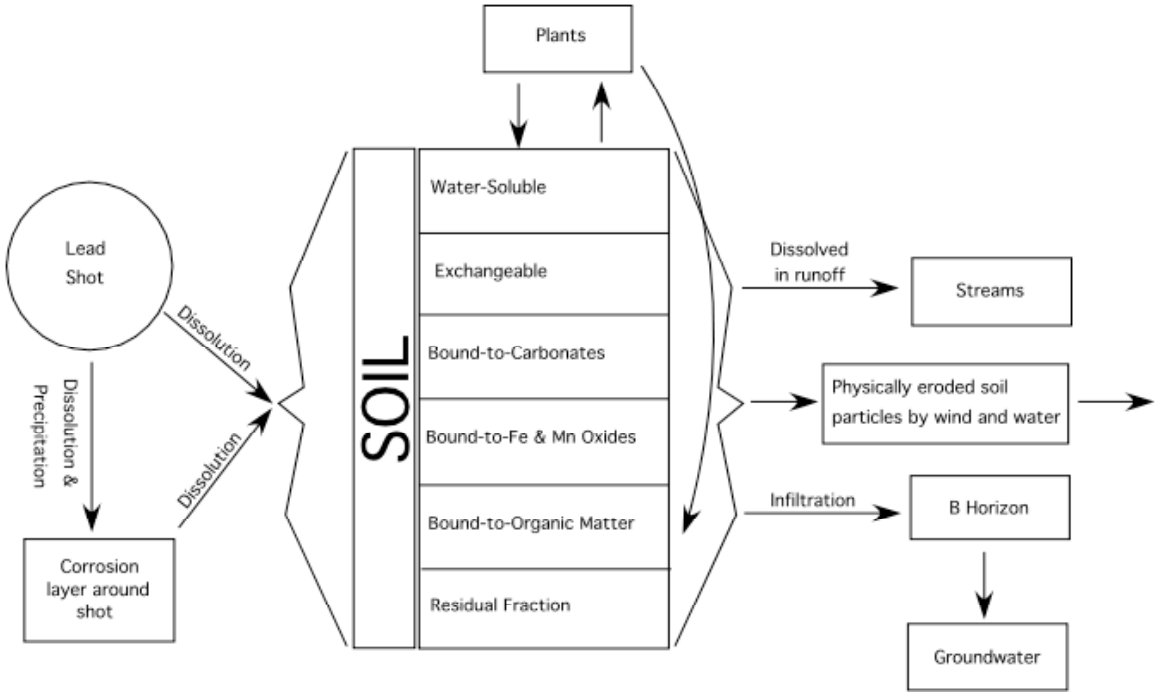

Figure 1. Pathways and reservoirs for lead on shooting ranges. Arrows represent pathways and boxes represent reservoirs.

MATERIALS AND METHODS

This study was conducted at the U.S. Department of Agriculture Forest Service shooting range facility, located in the Jefferson National Forest approximately 5 km west of Blacksburg, VA (37°17' 26" N, 080°27' 28" W); see Figure 2. The facility consists of two ranges, a rifle/pistol range and a shotgun range established on the southeastern flank of Sinking Creek Mountain (Craig 1999). The rifle range lies 100 m northwest of the shotgun range. An unnamed intermittent tributary to Craig Creek, a tributary of the James River, runs between the two ranges and receives runoff from the shotgun range. Runoff

from the rifle range is collected in a small retention pond that drains into a different tributary of Craig Creek, Figure 2. The ranges are constructed in the Berks-Weikert soil complex, which is composed of shaly silt loam soil (USDA 1980), developed on the Devonian-aged Brallier formation, which is a deeply weathered black shale (Craig 2002). Silurian-aged sandstone float stones from the adjacent ridge top occur throughout both ranges. The shotgun range was selected for our research due to the broad distribution of lead shot on the range, as opposed to the rifle/pistol range, where lead tends to concentrate in the berms and backstops immediately behind the target locations. A 60 m by 60 m previously forested area that has been cleared, graded and is now covered with grass, defines the developed part of the shotgun range. The range is completely surrounded by the Jefferson National Forest. A previous study reports that lead shot was recovered at distances as far as 300 m from the designated shooters box and that more than 80% of the spent shot lies beyond the 60 m by 60 m cleared area (Craig 2002). The locations of the 17 soil core samples collected from the developed part of the range are shown in Figure 3. The Jefferson National Forest shooting range facility is an exceptional research site due to its isolated geographical location, which eliminates the possibility of lead contamination from external sources. Five background samples were collected from two locations that are not influenced by shooting range activity. The background samples were collected from a grassy area adjacent to the road leading up to the shooting ranges and from a forest service access road locate 0.5 km beyond the entrance to the shooting range on Craig Creek Road. The shooting range facility, has seen continual usage since its opening in 1993 and is anticipated to remain operational for the immediate future (Craig 2002).

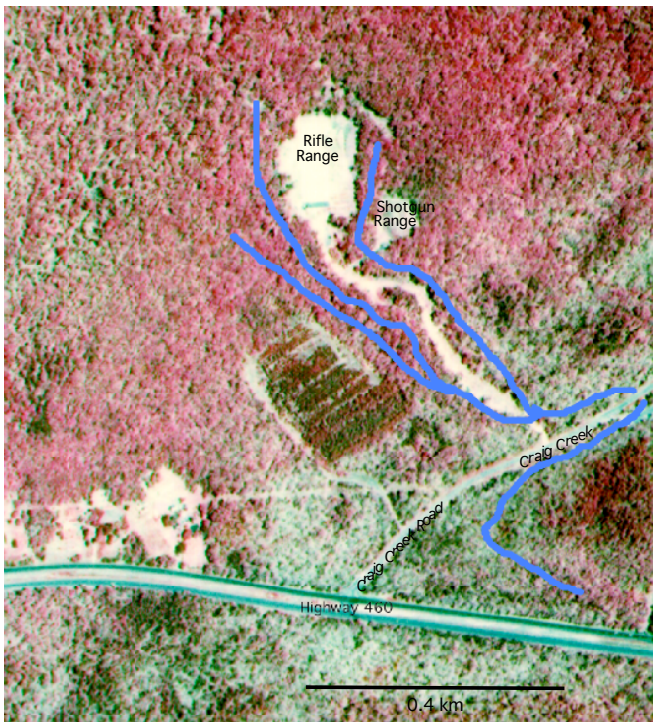

Figure 2. The shooting range is located in the Jefferson National Forest approximately 5 km west of Blacksburg, Virginia. The shooting range facility is drained by tributaries of Craig Creek.

Soil samples from the shotgun range and background sites were collected with a soil recovery probe and slide hammer. The soil recovery probe was hammered to a depth of as much as 1 meter to guarantee a recovered soil core length of at least 50 cm. The soil

cores were collected in 7/8-inch diameter by 24-inch long butyrate plastic cylinder liners that load into the soil recovery probe. New butyrate plastic liners were used for each soil core collected. The plastic liners were spilt and the soil cores were dissected into four depth profiles: surface to A-horizon, A-horizon to 10 cm, 10 to 30 cm, and 30 to 50 cm. The soil sampling protocol is given in Appendix 1. The base of the A-horizon was identified by the transition from an organic-rich, darker layer to an underlying clay-rich, yellowish to orange layer (Craig 2002). Due to the grading of the range and background sites it is likely that the original soil structure of the Berks and Weikert soil complex has been altered, obliterated, or at least the thickness of the original A-horizon has been reduced. The four depth profiles were separated into plastic storage containers and air-dried in a forced air oven at 50 ° C for a minimum of 6 hours. After complete drying, each sample was disaggregated and visually inspected for the presence of any shot and or bullets. Visible shot and or bullets were removed and discarded. The samples were then pulverized with a mortar and pestle and sieved through a 2 mm stainless steel sieve. The sieved soil samples were reserved for later selective sequential extractions (SSE).

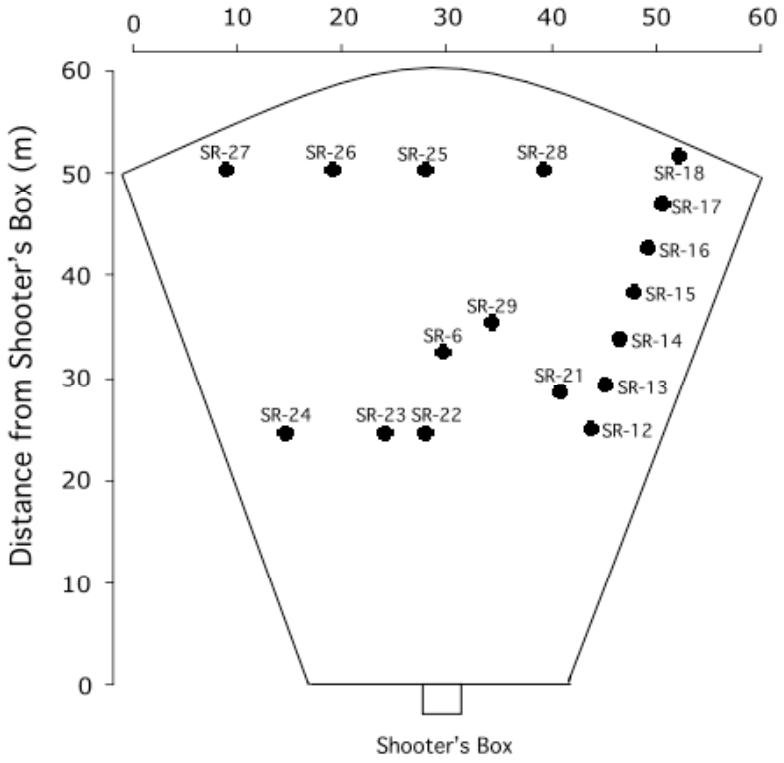

Figure 3. Sample locations of soil cores collected from the shotgun range.

Selective sequential extractions (SSE) were conducted to identify the reservoirs of mobile lead in the shooting range soil. Using SSE methodology developed by Tessier (1979), and later modified by Ma (1997), lead was extracted as five fractions: water soluble, exchangeable, bound-to-carbonates, bound-to-Fe and Mn oxides, and bound-to-organic matter. The final extraction step of the SSE method, the residual fraction, was not extracted and analyzed due to the low solubility of the remaining lead silicates, lead phosphates, and other lead constituents.

The protocol used for the SSE is given in Appendix 2. In summary, the five fractions were obtained as follows:

1. Water-Soluble Fraction: One gram of soil was extracted with 15 mL of deionized water for 2 hours with continuous agitation by a wrist action shaker.

2. Exchangeable Fraction: The residue from the previous extraction was extracted with 8 mL of 1 M $MgCl_2$, (pH 7) for 1 hour with continuous agitation with a wrist action shaker.

3. Bound-to-Carbonates Fraction: The residue from the previous extraction was extracted with 8 mL of 1 M $NaCH_3COO$ adjusted to pH 5 with CH_3COOH for 5 hours with continuous agitation with a wrist action shaker.

4. Bound-to-Fe & Mn Oxides Fraction: The residue from the previous extraction was extracted with 0.04 M $NH_2OH•HCl$ in 25% v/v CH_3COOH at 96° C for 6 hours with occasional agitation by hand.

5. Bound-to-Organic Matter Fraction: The residue from the previous extraction was extracted with a combination of 3 mL 0.02 M HNO_3 and 5 mL of 30% H_2O_2 adjusted to pH 2 with HNO_3 at 85° C for 2 hours with occasional agitation by hand. After 2 hours, 3 mL of 30% H_2O_2 adjusted to pH 2 was added to the extracting solution and heated at 85° C for 3 more hours. After cooling to room temperature, 5 mL of 3.2 M NH_4OAc in 20% v/v HNO_3 was added and the resulting extracting solution was diluted to 20 mL with deionized water and agitated continuously with a wrist action shaker for 30 minutes. Separation of the solids after each successive extraction was completed by centrifuging the sample in an anglehead rotor at 2750 rpm (930 x g) for 30 minutes. The resulting supernatants were decanted and filtered with 0.2 μm nylon, 25 mm diameter syringe filters. All supernatants samples were acidified with 5 drops of 1:10 HNO_3 and stored in a refrigerator until analysis. Prior to the next extraction, 8 mL of deionized water was added to each residue, agitated by hand, centrifuged for 30 min, decanted, and discarded.

Lead concentrations in the extracted supernatants were determined by inductively coupled plasma-atomic emission spectroscopy (ICP-AES), on a SpectroFlame Modula

Tabletop ICP with auto-sampler type: FTMOA85D at the Virginia Tech Soil Testing Laboratory. The measurements were conducted at 168.220 nm wavelength. The ICP-AES was used for the analysis of lead concentrations because of its broad range of detection. The reported detection limit for the ICP-AES was 0.026 ppm. During statistical analysis, below detection limit values were treated as half of the reported detection limit. Total lead concentrations of each A-horizon soil sample was determined by XRAL Laboratories in Toronto, Canada using a Na_2O_2 fusion and ICP analysis. Soil pH measurements were conducted with a Ag-AgCl combination electrode at a 1:10 soil to deionized water ratio stirred for 1 hour or until pH stabilized.

All chemical reagents used in the extraction procedure were of analytical grade or better. All extraction solutions were analyzed to identify any lead that existed prior to the extraction procedure. All extractions were conducted in 1:10 HNO_3 washed polycarbonate labware. All supernatants were stored in 1:10 HNO_3 washed HDPE plastic sample bottles.

X-ray diffraction (XRD) was used to determine the predominant corrosion phase observed on the surface of the lead shot. One hundred grams of lead shot, recovered from the Blacksburg shotgun range, were submerged in deionized water, placed in the ultrasonic bath, and sonified for 20 minutes. The debris dislodged from the surface of the shot was decanted and collected on filter paper. The debris was powdered using a mortar and pestle and mounted on zero background quartz slides. Clay pigeon pieces collected from the shotgun range were powdered with a mortar and pestle and mounted on zero background quartz slides. Powder XRD patterns were taken on a Scintag XDS 2000 θ-θ goniometer, flat plate sample holder, powder diffractometer using an energy sensitive

solid-state detector. The incident beam slit size was 2 mm and the diffracted beam was 0.5 mm. The Cu K-α 1 wavelength was 1.5405 Å and the Cu K-α 2 wavelength was 1.54439 Å. All samples were scanned at 1°/min from 5 to 60 degrees 2θ and spun to decrease the likelihood of preferential orientation in the powder mounts.

RESULTS

Mineralogy

White corrosion spots were observed on the surfaces of shot recovered from the shotgun range. This corrosion was removed from the shot surface by the ultrasonic bath treatment. X-ray diffraction analysis identified hydrocerussite ($Pb_3(CO_3)_2(OH)_2$) as the predominate mineral phase in this removed material. Hydrocerussite has also been identified as the primary corrosion phase on shot and bullets collected at a number of other sites (Jorgensen 1987; Lin 1995; Lin 1996; Chen 2002; Cao 2003). Samples of clay pigeon material collected from the shotgun range, analyzed by XRD, contain ankerite ($Ca(Mg,Fe)(CO_3)_2$).

Selective Sequential Extraction (SSE) Results

All SSE results are presented in Appendix 3. The pattern of lead concentrations in the samples collected from the range were tested for normal distribution in the five extracted soil fractions, water-soluble, exchangeable, bound-to-carbonates, bound-to-Fe and Mn oxides, and bound-to-organic matter using the Shapiro-Wilk W test from statistical analysis software, JMP Version 2 (Sall 1989). None of the soil fractions showed a normal distribution of lead concentrations, but rather they showed extended

tails to the higher concentration levels. The Shapiro-Wilk W test showed that concentration data for all of the soil fractions except the bound-to-organic matter fraction were log-normally distributed. Therefore, the entire data set was analyzed as if the data were log-normally distributed. Thus the geometric mean concentrations are reported rather than arithmetic mean concentrations.

Figure 4 shows the geometric mean lead concentration of the shotgun range soil and background soil in mg/kg for each soil fraction and each profile sampled. The shotgun range lead concentrations were computed using the data from the 17 soil core samples collected from the developed portion of the shotgun range. The background lead concentrations were computed from five soil core samples collected from two non-forested areas adjacent to the shotgun range that are not impacted by shooting activities on the shotgun range.

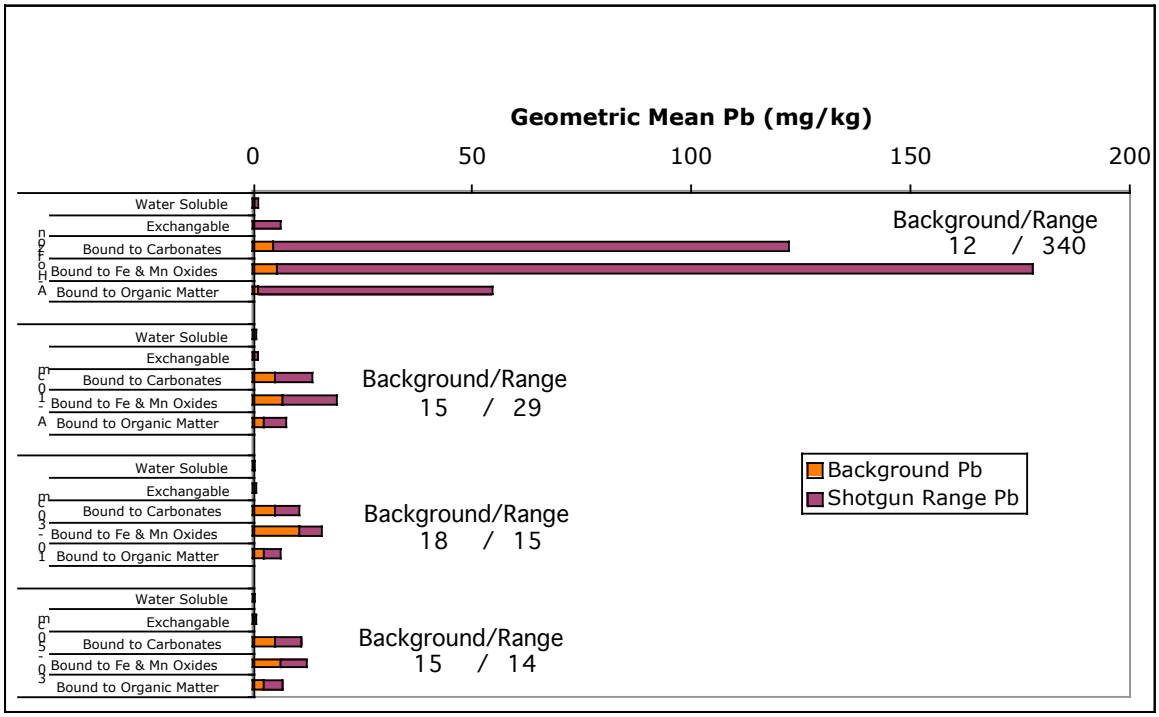

Figure 4. Geometric mean Pb concentrations (mg/kg) for each soil fraction verses depth. Totals (sum of all lead concentration in all fractions) for background and shotgun range extractable lead concentrations are given to the right of each depth profile.

Distribution of A-horizon extractable Pb vs. Surface Pb shot concentration

The relationship between extractable lead concentrations and lead shot concentrations on the shotgun range (Craig 2002) are compared in Figure 5. The zero value on the x-axis is the location of the shooters box. The highest concentration of spent shot, 5 kg/m^2, was observed at 28 m immediately in front of the shooters box. The kriging routine used by Craig (2002) smoothed this peak to around 3 kg/m^2. These diagrams were created using the kriging routine of the Surfer software package (Golden Software 1999).

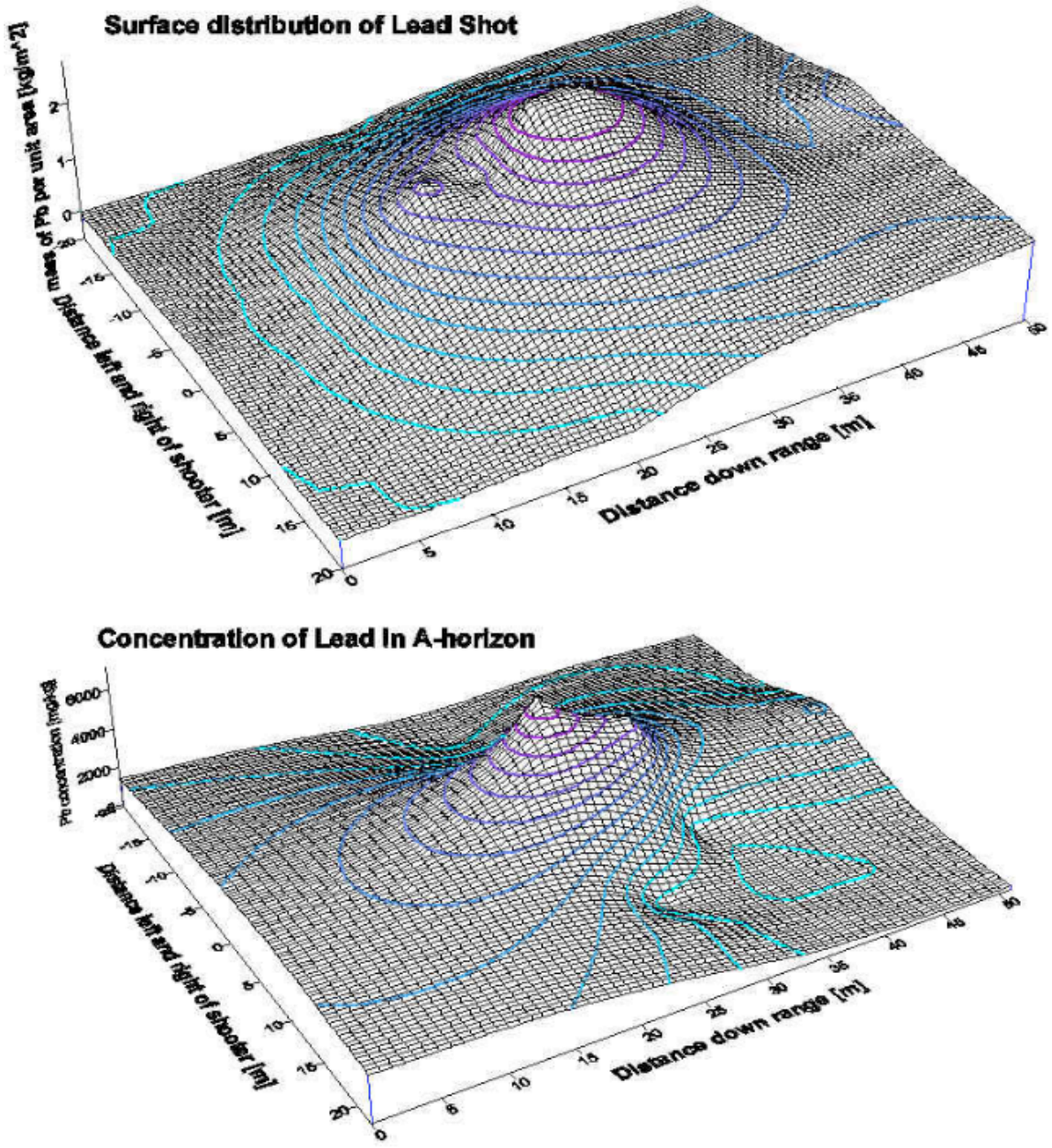

Figure 5 a. (top), The mass of shot per unit area on the surface of the shotgun range as reported by (Craig 2002), 5 b. (bottom), is the total extractable lead measured in the A-horizon. The contour intervals for shot concentrations are 0.1 kg/m^2 (Figure 5a), and the contour intervals for the extractable lead concentrations are 100 mg/kg (Figure 5b).

Water Solubility

Figure 6 shows the lead concentrations and pH values of the deionized water-soluble lead concentrations for the A-horizon and surface water samples collected from the shotgun range. The data were censored to remove any lead concentrations that were below detection limits (BDL) of the ICP. The data points are plotted on solubility diagrams for hydrocerussite and cerussite. Four solubility curves are plotted on each diagram using four different total carbonate values, 10^{-4} m, 10^{-3} m, 10^{-2} m, and 10^{-1} m.

DISCUSSION

Mineralogy

Hydrocerussite was the only corrosion product in the shot coating identifiable in the XRD analysis. Cerussite ($PbCO_3$), massicot (PbO), and anglesite ($PbSO_4$), which were identified in shot corrosion coatings by Jorgensen (1987), Lin (1995), Lin (1996), Chen (2002), Cao (2003), and Cao (2003), were not distinguishable from the background in the XRD analysis.

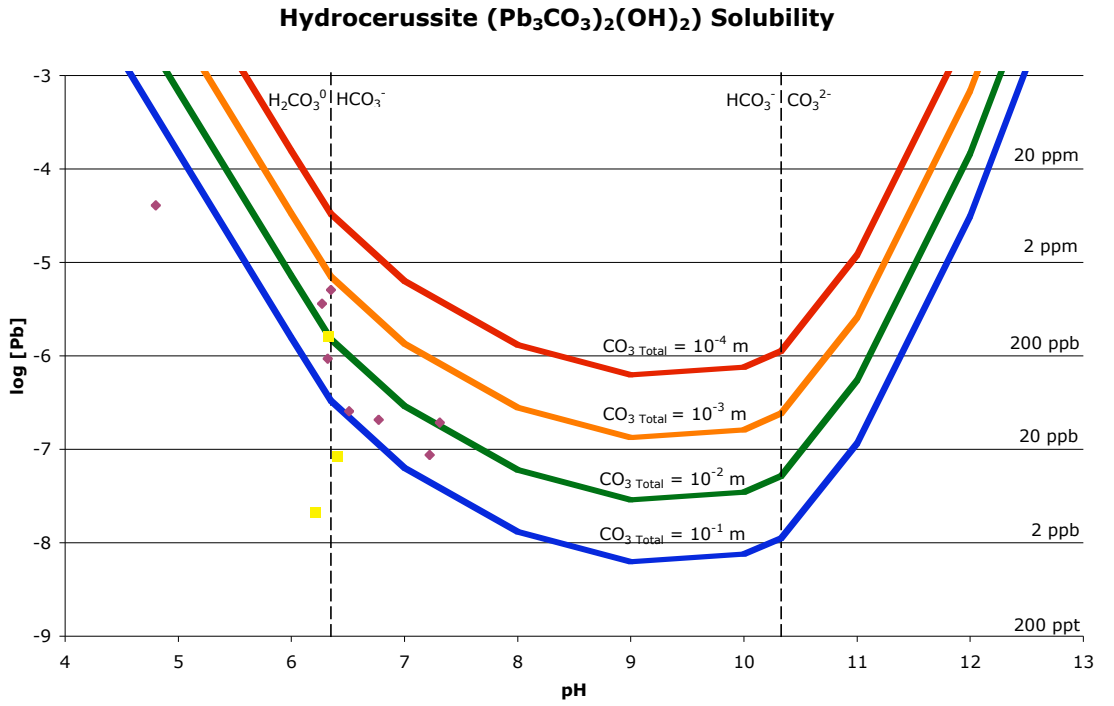

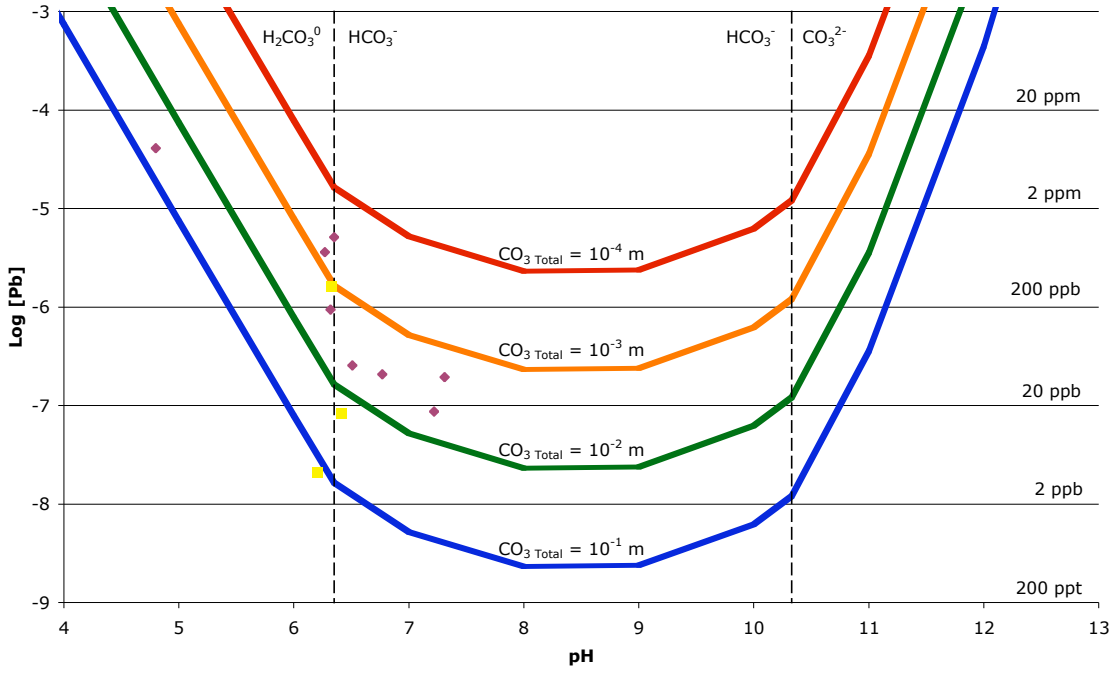

Figure 6. Lead concentrations (mg/kg) and pH values for deionized water equilibrated with A-horizon soil samples (diamonds) and surface water samples collected from the

shotgun range (squares) (Craig 1999) plotted on a graph showing the solubility of hydrocerussite (top) and cerussite (bottom) (thermodynamic data from Schock (1996)).

The Eh-pH diagram (Figure 7) for the Pb-CO_3-H_2O system is useful in interpreting the mineralogy of the shot coatings. Figure 7 shows that cerussite should be the stable lead phase at the pH value of the A-horizon soils. This figure was created using a total carbonate concentration of 10^{-2} m, which fit the water-soluble extraction data for hydrocerussite in Figure 6 extremely well and an average lead concentration of 10^{-6} m. Thermodynamic data presented by Schock (1996) were used to construct the diagram. Free energy values used to create the Eh-pH diagram are given in Appendix 4. More recent free energy data for hydrocerussite were published by Mercy (1998), ΔG_R = -1699.8 kJ/mol, but the more negative ΔG_R for hydrocerussite, ΔG_R = -1710.84 kJ/mol, reported by Schock (1996), is more consistent with our observations because it predicts a larger stability field for hydrocerussite.

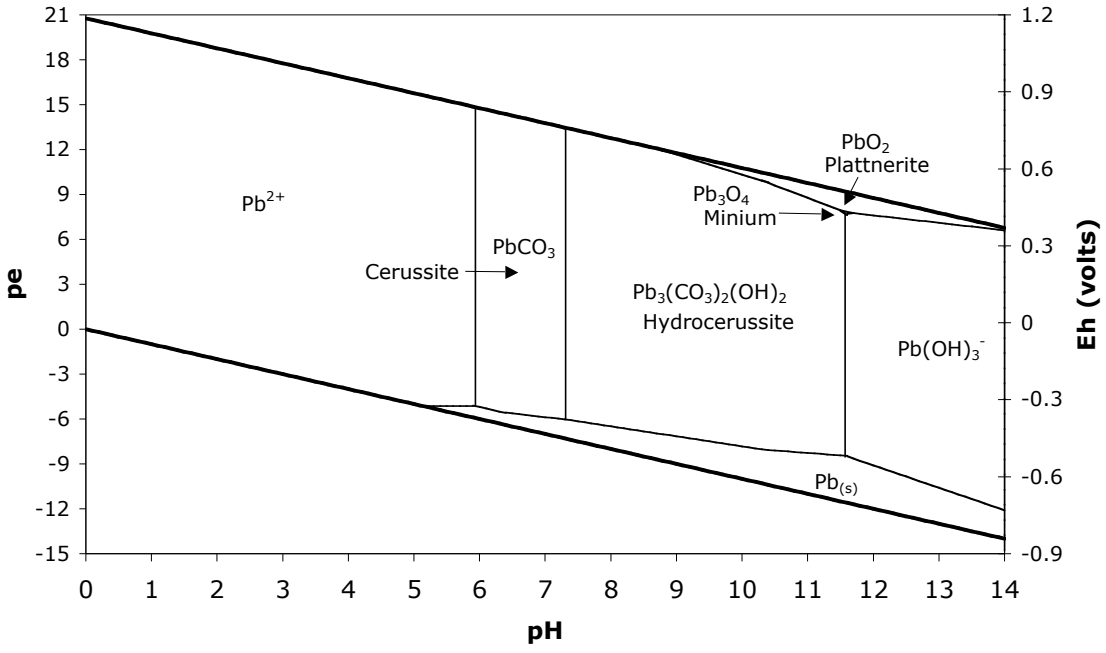

Figure 7. Eh-pH diagram for the Pb-CO_3-H_2O system at 25° C and 1 atm, [Pb] = 10^{-6} m, and [CO_{3Total}] = 10^{-2} m.

Metallic lead is stable at low redox potentials and slightly acidic to extremely basic pH conditions. As metallic lead corrodes it consumes both oxygen and hydrogen ions, $Pb_{(s)} + 0.5O_2 + 2H^+ = Pb^{2+} + H_2O$, thus the environment at the metal's surface is expected to have a low Eh and high pH. The lead oxidation product hydrocerussite, which was identified as the corrosion product on the surfaces of shot collected from the shotgun range, is stable at low Eh and high pH conditions, (Figure 7). Based on the free energy values the first oxide likely to be formed when lead is exposed to the atmosphere is litharge (PbO) Graedel (1994) but litharge has never been reported as a corrosion phase associated with corroding lead shot and bullets. Massicot (PbO), which has a nearly identical free energy value to litharge (Appendix 4) is frequently reported as a corrosion phase associated with the corrosion of lead shot and bullets (Lin 1996; Chen 2002; Cao

2003; Cao 2003). Massicot, which does not appear on the Eh-pH diagram shown in Figure 7, is stable at higher lead concentrations and/or lower total carbonate concentrations. At lower carbonate concentrations a stability region for lead oxides occurs on the right hand side of the Eh-pH diagram. Corrosion of the metallic lead will continue until a more stable corrosion product, like hydrocerussite, coats the surface, in effect passivating the shot and reducing the corrosion rate (Graedel 1994; Black 1999). The corrosion layer limits the transport of H^+ and $O_{2(g)}$ to the bullet's surface. Beccaria (1982) found hydrocerussite to be a primary phase that passivates lead in seawater under stagnant conditions. Lin (1996) observed a massicot corrosion layer between a lead pellet and the outer hydrocerussite corrosion layer. The hydrocerussite corrosion layer not only limits the rate of H^+ and $O_{2(g)}$ to the metal surface, but it also traps the soluble lead near the shot surface so lead concentrations increases until massicot becomes stable. All of these corrosion products are soluble in acidic environments (Figure 7), and this promotes the rapid dissolution of shot at low pH (Jorgensen 1987).

It is possible that cerussite, though not present as a corrosion product on the surfaces of the lead shot, is present in the soil (Figure 7). The lead concentrations in the deionized water extractions of the A-horizon soils (Figure 6) are consistent with the solubility patterns of both cerussite and hydrocerussite. Furthermore, the amount of lead carbonate minerals in the soil samples is far too low to produce an X-ray diffraction pattern. Fortunately both of these minerals have similar solubility patterns so the same best management practices apply regardless of which phase is present.

A predominant component of the clay pigeons used as aerial targets on the shotgun range was identified by XRD analysis as ankerite, a Ca, Fe, and Mg carbonate.

Coal-tar pitch or petroleum pitch is used to bind the powdered carbonate into discs. Baer (1995) reported the composition of new clay pigeon targets as 67% dolomitic limestone, 32% petroleum pitch, and 1% fluorescent aqueous paint (painted targets only). The breakdown and decomposition of the clay pigeons releases carbonate and increases the surface soil pH, which lowers the solubility of hydrocerussite and cerussite. The average A-horizon soil pH of the shotgun range is almost one unit higher than the average soil pH for the corresponding background A-horizon, (Table 1). All pH results are presented in Appendix 5. Below the A-horizon the average shotgun range soil pH's and the average background soil pH's are similar. It is also possible that some of the increase in the shotgun range soil pH is due to hydrogen ion consumption by the corrosion of metallic lead.

Table 1. Average soil pH's for shotgun range and background sample verses depth, ± is equal to one standard deviation.

Horizon Depth	Average Shotgun Range Soil pH	Average Background Soil pH
A-horizon	6.65 ± 0.82	5.81 ± 0.19
A-10 cm	5.41 ± 0.74	5.41 ± 0.36
10-30 cm	4.76 ± 0.53	4.85 ± 0.28
30-50 cm	4.54 ± 0.20	4.60 ± 0.30

Selective Sequential Extraction Results

Figure 4 clearly indicates that the majority of the extractable lead is present in the A-horizon. The total extractable lead is the sum of the extractable lead that could be available under natural conditions in the water soluble, exchangeable, bound-to-carbonates, bound-to-Fe and Mn oxides, and bound-to-organic matter soil fractions. The total extractable lead in the next lower (A-10 cm) horizon is only about 5% of the amount

found in the A-horizon. The deeper horizons, 10-30 cm and 30-50 cm, contain background total extractable lead levels. Because of the low solid to solution ratio of the extraction procedures it is possible that extracts from samples with high lead concentrations could have become saturated with respect to lead during the extraction, making total extractable lead concentrations an underestimate. For, example we believe that the water extraction lead concentrations represent equilibrium with a lead carbonate or hydroxycarbonate solid phase. Repeated extractions with water should continue to show similar lead concentrations until all of the lead bearing mineral has been dissolved.

The total lead concentrations (extractable and non-extractable) for the A-horizon soil are given in Appendix 6. The total lead concentrations are higher than that of the total extractable lead concentrations, because there is lead present in feldspars, phosphate, and zircon minerals, and in metallic fragments. Structurally contained lead and metallic lead fragments are not accounted for in the total extractable lead concentration, however this lead is not mobile on the short timescale of the extraction tests. It can become mobile only as the result of long-term weathering or corrosion reactions.

The soil and the individual soil fractions are significant reservoirs for the lead released by the shot corrosion (Figure 1). The bound-to-Fe and Mn oxide fractions and bound-to-carbonate soil fractions contained the majority of the extractable lead in both the shotgun range and background soil samples in all of the depth horizons. It is not surprising that the bound-to-Fe and Mn oxide soil fraction contains the most extractable lead. Lead is an easily hydrolyzed metal, which strongly adsorbs to oxide and hydroxide soil minerals at typical soil pH's (Mckenzie 1980). On the shotgun range, the A-horizon soil pH values range from 4.80 to 7.39, which fall into the stability field for cerussite on

the Eh-pH diagram (Figure 7). This suggests that a significant amount of lead is either present as cerussite, hydrocerussite, or as part of carbonate solid solution. Rimstidt (1998) reported an effective K_D for lead in calcite of around 17. Godelitsas (2003) found that lead was rapidly removed from an aqueous solution and precipitated on the surface of various size calcium carbonate fragments and crystals as cerussite and hydrocerussite. The bound-to-organic matter soil fraction also showed a significant extractable lead level in the A-horizon. Rickard (1978) reported that humic and fulvic acids have a large binding capacity for lead. Because the surface to A soil horizon contains a significant quantity of soil organic matter it is not surprising to see high bound-to-organic matter extractable lead concentrations in there. The water-soluble and exchangeable soil fractions contained relatively little extractable lead when compared to the bound-to-Fe and Mn oxide and bound-to-carbonate soil fractions. The location of the seventeen samples collected from the developed portion of the range exhibit a bias to the right-hand side of the range, (Figure 3). The value of total extractable lead in the A-horizon might be slightly higher if this bias was removed, but the pattern of significant concentrations of the extractable lead found in the A-horizon, low extractable lead in the A-10 cm horizon, and background lead levels below 10 cm depth, would be similar.

Distribution of A-horizon Extractable Pb versus Surface Pb Shot Concentration

Figure 5 shows the lead concentration found in the A-horizon as a function of sample location on the range. These concentrations correlate well with shot concentrations reported by Craig (2002). These figures show that there is a positive correlation between the total mass of shot deposited on the range and the amount of total extractable lead found in the A-horizon. The data for the three deeper horizons, A–10 cm,

10–30 cm, and 30–50 cm, show no such correlation. These results clearly show that the high extractable lead concentrations in the soil are the result of lead released from the corrosion products on the shot. Furthermore they also show that there is little or no lateral or vertical dispersion of the lead beyond the locality where the shot are corroding. This identifies the A-horizon soil as a significant barrier to lead migration.

Water Solubility

The solubility's of hydrocerussite and cerussite are strongly pH dependent, both with a minimum solubility near pH 9 (Figure 6). A decrease in pH from 8 to 5 will increase hydrocerussite's solubility by four orders of magnitude and cerussite's solubility by three orders of magnitude. The dissolved lead concentrations in the deionized water extraction from the A-horizon data are plotted on Figure 6 to show that either cerussite or hydrocerussite could be controlling the dissolved lead concentration in soil pore waters and in runoff at this site. The datum for sample SR-6 was not plotted on this diagram because the large amount of crushed clay pigeon material observed in this sample likely affected the pH of the extract, making it more basic than soil typically observed on the shotgun range. The total carbonate contour of 10^{-2} m for hydrocerussite follows the water-soluble extractable lead trend. A total carbonate contour of $10^{-2.5}$ m for cerussite would also fit the water-soluble extractable lead trend. It is impossible to determine which carbonate mineral, hydrocerussite or cerussite controls lead solubility in the shotgun range soil. Craig (1999) reported lead concentrations in surface waters hydrologicaly associated with this shooting range. A surface water sample collected at the location of SR-22 (Figure 3), had a lead concentration of 333 ppb. Surface water samples taken from pooled rainwater on the shotgun range had lead concentrations,

ranging from 4 to 333 ppb. Measured lead concentrations and pH's from surface waters were similar to those found in the deionized water-soluble extraction (Figure 6). It can be assumed that the deionized water-soluble extraction data represent the maximum lead concentrations attainable in surface water samples on the range because of the lengthy agitation period during the extraction. Craig (1999) also sampled Craig Creek, the stream that drains this range. Upstream of the shooting range where the stream is presumably not influenced by shooting range activities, the stream had a lead concentration of 0.5 ppb. Samples taken from 300 meters down stream of the shooting range had a lead concentration of 0.3 - 1.6 ppb. It is clear that the shooting range facility has little impact on Craig Creek.

Lead Mobility at Other Sites

Each shooting range has a specific ecological, climatic, and geochemical setting. This research was conducted at the Blacksburg, VA shotgun range and results obtained from this study are only applicable to this range and ranges with similar ecological, climatic and geochemical properties. However the protocol used for determining the dissolution, transport, and fate of lead on this shooting range should be applicable to all ranges. Shooting ranges in different settings will undoubtedly show different lead reservoirs and pathways (Figure 1), which mandates site-specific geochemical investigations. For example, shooting ranges on abandoned mine sites that have acidic sulfate soil/overburden will likely show higher dissolution rates of lead shot and bullets due to the acidity and significant lead sequestration in the form of anglesite ($PbSO_4$). Chlorides from salt spray could form lead hydroxychloride corrosion products on shot found on shooting ranges adjacent to marine environments (Graedel 1994). Environments

rich in organic matter will have acidic soils with dissolved organic compounds that can complex lead to promote significant dissolution and mobility of lead (Lin 1995).

BEST MANAGEMENT PRACTICES (BMP'S)

The geochemical study of the Blacksburg shooting range provides us with a framework for understanding of lead reservoirs and pathways at a typical shooting range. Based on this information we can suggest the following best management practices (BMP's), for this and similar sites. The implementations of BMP's on new and existing shooting ranges are vital to reducing the risk of lead migration off site.

The majority of the extractable lead is contained within the A-horizon of the soil, which is susceptible to erosion by both wind and water. Therefore it is essential that the range surface maintain a vegetative cover with grass or other plants that have substantial root systems to bind the soil particles and inhibit erosion.

Under no circumstances should plants be cultivated for consumption by humans or animals on existing or formerly used shooting ranges. Plants growing on shooting ranges have been shown to have elevated lead concentrations in their roots and shoots (Mannien 1993; Mellor 1994; Rooney 1999; Hui 2002; Lee 2002; Mozafar 2002), see Figure 1. Domestic animals must also be restricted from grazing on existing or formerly used shooting ranges. (Braun 1997) reported lead poisoning of calves pastured on a military shooting range. This project did not evaluate whether consumption of plants growing on shooting ranges by wildlife might furnish a significant pathway for lead transport off the range.

Nriagu (1973, 1974) reports that in the presence of sufficient amounts of phosphate, lead can be immobilized as pyromorphite ($Pb_5(PO_4)_3OH$) or chloropyromorphite ($Pb_5(PO_4)_3Cl$). Pyromorphite and chloropyromorphite are extremely insoluble and can effectively render lead in soil imobile. Previous researchers (Ma 1993; Ruby 1994; Ma 1995; Ma 1997; Zhang 1999; Melamed 2003) have added rock phosphate and hydroxyapatite to contaminated soils to reduce the bioavailability of lead. Even though the lead on this range is strongly held by the bound-to-carbonate and bound-to-Fe and Mn oxides soil fractions and therefore has no significant mobility in infiltrating waters, the addition of phosphate would be an additional preventative measure to limit lead mobility.

The addition of pulverized limestone to the surface of the Blacksburg shotgun range will raise the soil pH and increase the total carbonate concentration. An increase in soil pH will reduce the corrosion rate of the lead shot and bullets by lowering the availability of H^+ ions. Raising the soil pH also has the effect of reducing the solubility of hydrocerussite and cerussite. Hydrocerussite and cerussite have minimum solubility's near pH 9. The addition of pulverized limestone to the range surface cannot raise the soil pH this high because the equilibrium pH of calcite, solution, and air with P_{CO2} of $10^{-3.5}$ is near 8.3 (Faure 1998). However, the pH of the surface soil should not be raised so high that it will adversely affect the plant species that are growing on the range. The addition of pulverized limestone to the range will also increase the potential lead sorbing reservoir of the bound-to-carbonate soil fraction, resulting in increased capacity to limit lead mobility.

Soil stabilization is also important in reducing physically eroded soil particles. Tilling or gradingwill move lead to deeper soil horizons, improve water infiltration, aerate the soil, and destroy the protective vegetation cover on the range, all of which encourage lead transport dispersion. Jorgensen (1987) reported that lead shot on a Danish shotgun range corroded faster in cultivated soil than on natural or grassland soils. At the Blacksburg shotgun range where the range surface has not been tilled, the extraction data showed that there was no significant downward lead movement beyond 10 cm. Agricultural tillage could extend lead contamination to depths of 20 cm or more. Even in the sample SR-22 which corresponded to the highest concentration of surface lead observed by Craig (2002), minimal concentrations of lead are observed below the A-10cm horizon (Figure 8). Tilling of the surface will also make the potential recovery of the lead shot and bullets by a salvage recycling company much more difficult and costly.

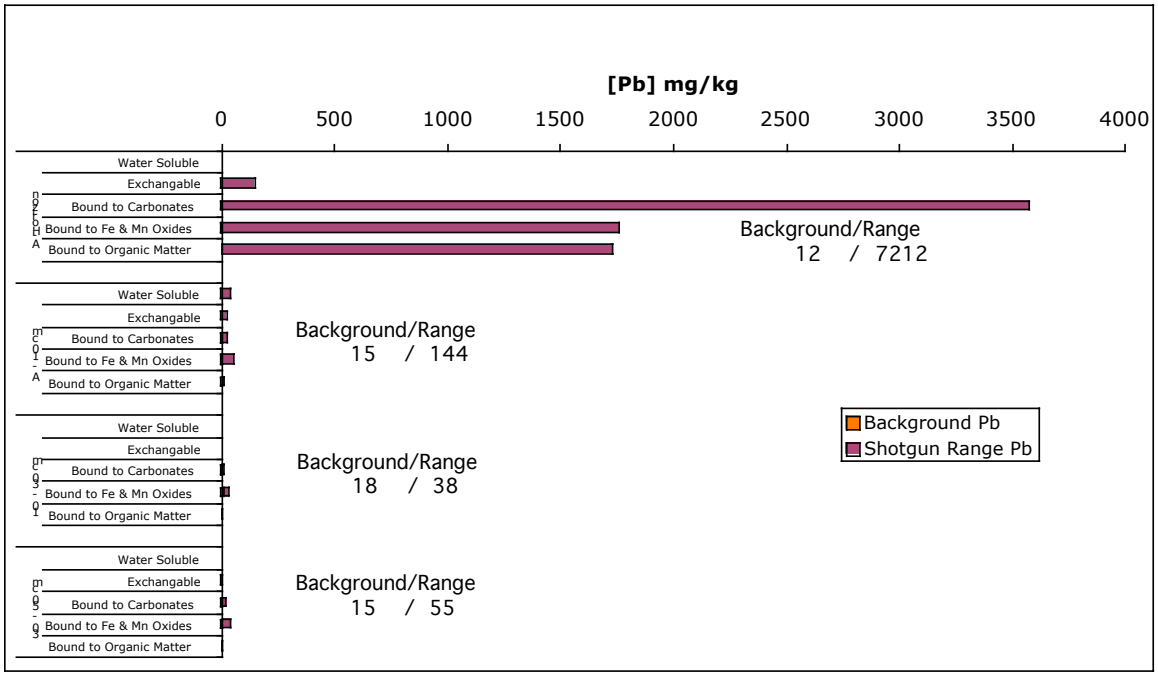

Figure 8. SR-22 Lead concentrations (mg/kg) and geometric mean background Pb concentrations (mg/kg) for each soil fraction vs. depth. Totals for background and shotgun range extractable lead concentrations are given to the right of each depth profile.

The transport of physically eroded of soil particles by precipitation runoff (Figure 1) should be minimized. A retention pond should be constructed immediately down gradient of the range to collect surface runoff eroded soil particles and prevent them from entering any surrounding streams or rivers. In addition any dissolved lead will collect in the retention pond and precipitate out as cerussite or hydrocerussite or be sorbed to the sediments in the retention pond.

REFERENCES

Astrup, T., J. K. Boddum, and T. H. Christensen (1999). "Lead distribution and mobility in a soil embankment used as a bullet stop at a shooting range." Journal of Soil Contamination **8**(6): 653-665.

Baer, K. N., D.G. Hutton, R.L. Boeri, T.J. Ward, and R.G. Stahl, Jr (1995). "Toxicity evaluation of trap and skeet shooting targets to aquatic test species." Ecotoxicology **4**(385-392).

Basunia, S., and S. Landsberger (2001). "Contents and leachability of heavy metals(Pb, Cu, Sb, Zn, As) in soil at the Pantex firing range, Amarillo, Texas." Journal of Air & Waste Management Association **51**(10): 1428-1435.

Beccaria, A. M., E.D. Mor, G. Bruno and G. Poggi (1982). "Corrosion of lead in sea water." British Corrosion Journal **17**(2): 87-91.

Black, L., and G.C. Allen (1999). "Nature of lead patination." British Corrosion Journal **34**(3): 192-197.

Braun, U., N. Pusterla, and P. Ossent (1997). "Lead poisoning of calves pastured in the target area of a military shooting range." Schweizer Archiv Fur Tierheilkunde **139**(9): 403-407.

Bruell, R., N. P. Nikolaidis, and R. P. Long (1999). "Evaluation of remedial alternatives of lead from shooting range soils." Environmental Engineering Science **16**(5): 403-414.

Cao, X., L. Q. Ma, M. Chen, D. W. Hardison Jr., and W. Harris (2003). "Lead transformation and distribution in the soils of shooting ranges in Florida, USA." The Science of the Total Environment **307**: 179-189.

Cao, X., L. Q. Ma, M. Chen, D. W. Hardison Jr., and W. Harris (2003). "Weathering of lead bullets and their environmental effects at outdoor shooting ranges." Journal of Environmental Quality **32**: 526-534.

Chen, M., L. Q. Ma, and W. G. Harris (2001). "Distribution of Pb and As in soils at a shooting facility in central Florida." Soil and Crop Sciences Society of Florida Proceedings **60**: 15-20.

Chen, M., S. Daroub, L. Ma, W. Harris, and X. Cao. (2002). "Characterization of lead in soils of a rifle/pistol shooting range in central Florida, USA." Soil and Sediment Contamination **11**: 1-17.

Craig, J. R., D. Edwards, J. D. Rimstidt, P. F. Scanlon, T. K. Collins, O. Schabenberger, and J. B. Birch. (2002). "Lead distribution on a public shooting range." Environmental Geology **41**: 873-882.

Craig, J. R., J. D. Rimstidt, C. A. Bonnaffon, T. K. Collins, and P. F. Scanlon. (1999). "Surface water transport of lead at a shooting range." Bulletin of Environmental Contamination and Toxicology **63**: 312-319.

EPA (2001). Best management practices for lead at outdoor shooting ranges.

Faure, G. (1998). Principles and applications of geochemistry. Upper Saddle River, New Jersey, Prentice Hall.

Feierabend, J. S. (1983). "Steel shot and lead poisoning in waterfowl." National Wildlife Federation, Scentific and Technical Series **8**.

Godelitsas, A., J.M. Astilleros, K. Hallam, S. Harissopoulos, and A . Putnis (2003). "Interaction of calcium carbonates with lead in aqueous solutions." Environmental Science and Technology **37**: 3351-3360.

Golden Software, I. (1999). Surfer. Golden, Colorado, Golden Software, Inc.

Graedel, T. E. (1994). "Chemical mechanisms for the atmospheric corrosion of lead." Journal of Electrochemical Society **141**(4): 922-927.

Hui, C. A. (2002). "Lead distribution throughout soil, flora, and an invertebrate at a wetland skeet range." Journal of Toxicology and Environmental Health, Part A **65**: 1093-1107.

Jorgensen, S. S., and M. Willems (1987). "The fate of lead in soils: the transformation of lead pellets in shooting range soils." Ambio **16**(1): 11-15.

Knechtenhofer, L. A., I.O. Xifra, A.C. Scheinost, H. Fluher, and R. Kretzschmsar (2003). "Fate of heavy metals in a strongly acidic shooting-range soil: small-scale metal distribution and its relation to preferential water flow." Journal of Plant Nutrition and Soil Science **166**: 84-92.

Lee, I. S., O.K. Kim, Y.Y. Chang, B. Bae, H.H. Kim, and K.H. Baek (2002). "Heavy metal concentrations and enzyme activities in soil from a contaminated Korean shooting range." Journal of Bioscience and Bioengineering **94**(5): 406-411.

Lin, Z. (1996). "Secondary mineral phases of metallic lead in soils of shooting ranges from Orebro Country, Sweden." Environmental Geology **27**: 370-375.

Lin, Z., B. Comet, U. Qvarfort, and R. Herbert (1995). "The chemical and mineralogical behaviour of Pb in shooting range soils from central Sweden." Environmental Pollution **89**(3): 303-309.

Ma, L. Q., and G. N. Rao (1997). "Effects of phospate rock on sequential chemical extraction of lead in contaminated soils." Journal of Environmental Quality **26**: 788-794.

Ma, Q. Y., T.J. Logan, and J.A. Ryan (1993). "In situ immobilization of Pb by apatite." Environmental Science and Technology **27**: 1803-1810.

Ma, Q. Y., T.J. Logan, and J.A. Ryan (1995). "Lead immobilization from aqueous solutions and contaminated soils using phosphate rocks." Environmental Science and Technology **29**: 1118-1126.

Mannien, S. A. N., Tankanen (1993). "Transfer of lead from shotgun pellets to humus and three plant species in a finish shooting range." Archives of Environmental Contamination and Toxicology **24**: 410-414.

Mckenzie, R. M. (1980). "The adsorption of lead and other heavy metals on oxides of manganese and iron soil minerals." Australian Journal of Soil Researh **18**: 61-73.

Melamed, R., X. Cao, M. Chen, L. Q. Ma (2003). "Field assessment of lead immobilization in a contaminated soil after phosphate application." The Science of the Total Environment **305**: 117-127.

Mellor, A., and C. McCartney (1994). "The effects of lead shot deposition on soils and crops at a clay pigeon shooting site in northern England." Soil Use and Management **10**(3): 124-129.

Mercy, M. A., P. A. Rock, W. H. Casey, and M. M. Mokarram (1998). "Gibbs energies of formation for hydrocerussite and hydrozincite at 298 K and 1 bar from electrochemical cell measurements." American Mineralogist **83**: 739-745.

Mozafar, A., R. Ruh, P. Klingel, H. Gamper, S, Egli, and E. Frosard (2002). "Effect of heavy metal contaminated shooting range soils on mycorrhizal colonization of roots and metal uptake by leek." Environmental Monitoring and Assessment **79**: 177-191.

Murray, K., A. Bazzi, C. Carter, A. Ehlert, A. Harris, M. Kopec, J. Richardson, and H. Sokol (1997). "Distribution and mobility of lead in soils at an outdoor shooting range." Journal of Soil Contamination **6**(1): 79-93.

Nriagu, J. O. (1973). "Lead orthophosphates-II. Stability of chloropyromorphite at 25 degrees C." Geochemica et Cosmochimica Acta **37**(367-377).

Nriagu, J. O. (1974). "Lead orthophosphates-IV. Formation and stability in the environment." Geochemica et Cosmochimica Acta **38**(887-893).

Posner, H. S., T. Damstra, and J.O. Nriagu (1978). Human health effects of lead. The biogeochemistry of lead in the environment. J. O. Nriagu. Amsterdam, North-Holland Biomedical Press. **Part B:** 173-223.

Pott, D. B., B. K. Shepard, and A Modi (1993). "Lake Michigan sediment contamination from 73 years of trap and skeet shooting." Water Science and Technology **28**(8-9): 383-386.

Rickard, D. T. a. N., J.O. (1978). Aqueous environmental chemistry of lead. The Biogeochemistry of Lead in the Environment. J. O. Nriagu. Amsterdam, North-Holland Biomedical Press. **Part A:** 219-284.

Rimstidt, J. D., A. Balog, and J. Webb (1998). "Distribution of trace elements between carbonate minerals and aqueous solutions." Geochemica et Cosmochimica Acta **62**(11): 1851-1863.

Rooney, C. P., R. G. Mclaren, and R. J. Cresswell. (1999). "Distribution and phytoavailability of lead in a soil contaminated with lead shot." Water, Air, and Soil Pollution **116**: 535-548.

Rosen, J. F., and M. Sorell (1978). The metabolism and subclinical effects of lead in children. The Biogeochemistry of Lead in the Environment. J. O. Nriagu. Amsterdam, North-Holland Biomedical Press. **Part B:** 151-172.

Ruby, M. V., A. Davis, and A. Nicholson (1994). "In situ formation of lead phosphates in soils as a method to immobilze lead." Environmental Science and Technology **28**: 646-654.

Sall, J., Katherine Ng, and Michael Hecht. (1989). JMP. Cary, NC., SAS Institute Inc.

Sanderson, G. C. a. F. C. B. (1986). "Review of the problem of lead poisoning in waterfowl." Illinois Natural History Survey **Special Publication 4**: 1-34.

Schock, M. R., I. Wagner, and R. J. Oliphant (1996). Corrosion and solubility of lead in drinking water. Internal Corrosion of Water Distribution Systems**:** 131-230.

Tanskanen, H., I. Kukkonen, and J. Kaija (1991). "Heavy metal pollution in the environment of a shooting range." Geological Survey of Finland, Special Paper 12: 187-193.

Tessier, A., P. G. C. Campbell, and M. Bisson (1979). "Sequential extraction procedure for the speciation of particulate trace metals." Analytical Chemistry **51**: 844-851.

USDA (1980). Soil Survey of Montgomery Country Virginia, Soil Conservation Service.

Zhang, P., and J. A. Ryan (1999). "Transformation of Pb (II) from cerussite to chloropyromorhite in the presence of hydroxyapatite under varying conditions of pH." Environmental Science and Technology **33**: 625-630.

Appendix 1. Soil sampling and processing protocol.

Apparatus Needed

Soil core probe
Soil core probe liners
Soil core slide hammer
Labeled storage containers
Mortar and pestle
2 mm sieve

Soil Sample Collection Procedure

1. Record sample locations by referencing distance from the shooters box and the path down the center of the shotgun range.
2. Hammer the soil core probe at least 1 m into the ground to ensure retrieval of at least 50 cm of core.
3. Split plastic core liner and separate the sample into

   A-horizon (identifiable by color change from dark organic rich layer to yellowish clay layer)

   A-horizon to 10 cm

   10 cm to 30 cm

   30 cm to 50 cm
4. Dry in labeled plastic storage containers for six hours or until completed dry at 50°C in the forced air oven.
5. Remove all lead shot and bullets present.
6. Crush/pulverize the combined samples in a mortar and pestle.
7. Sieve the powdered samples through a stainless steel 2 mm sieve.
8. Collect 1 gram samples for each depth profile for sequential extraction.
9. Save remaining soil in labeled sealed plastic containers

Appendix 2. Selective Sequential Chemical Extraction protocol

Apparatus Needed

50 mL polypropylene centrifuge tubes
0.2 μm 25 mm nylon syringe filters
Centrifuge

Reagents Needed

Deionized water
1 M $MgCl_2 \cdot 6H_2O$ adjusted to pH 7 with 1:10 NaOH
1 M $CH_3COOHNa \cdot 3H_2O$ adjusted to pH 5 with CH_3COOH
0.04 M $NH_2OH \cdot HCl$ in 25% (v/v) CH_3COOH
0.02 M HNO_3
30% H_2O_2 adjusted to pH 2 with HNO_3
3.2 M CH_3COONH_4 in 20% (v/v) HNO_3

Extraction Procedure

Weigh 1 gram of processed soil for each depth, ex. A-horizon, A-10 cm, 10-30 cm, 30-50 cm.

Water Soluble Fraction

1. Extract 1 gram of soil with 15 mL of deionized water for 2 hours in a 50 mL polypropylene centrifuge tube, with continues agitation on the wrist action shaker.
2. Centrifuge the sample for 30 minutes at 2750 rpm.
3. Decant the supernatant, filter thru a 0.2 μm nylon syringe filter.
4. Add five drops of 1:10 HNO_3 to the sample. Store the sample in the refrigerator until ICP analysis.

5. Wash the residue with 8 mL of deionized water by vigorous hand shaking followed by 30 min in the centrifuge at 2750 rpm.
6. Decant and discard the supernatant. Save the residue for the next extraction step.

Exchangeable Fraction

1. Add 8 mL of 1 M $MgCl_2 \cdot 6H_2O$ at pH 7.0 to the residue collected from the previous water soluble fraction. Extract with continuous agitation on the wrist action shaker for 1 hour at room temperature.
2. Centrifuge the sample for 30 minutes at 2750 rpm.
3. Decant the supernatant, filter thru a 0.2 μm nylon syringe filter.
4. Add five drops of 1:10 HNO_3 to the sample. Store the sample in the refrigerator until ICP analysis.
5. Wash the residue with 8 mL of deionized water by vigorous hand shaking followed by 30 min in the centrifuge at 2750 rpm.
6. Decant and discard the supernatant. Save the residue for the next extraction step.

Bound-to-Carbonates Fraction

1. Add 8 mL of 1 M $CH_3COOHNa \cdot 3H_2O$ adjusted to pH 5.0 with CH_3COOH to the residue collected from the exchangeable fraction. Extract with continuous agitation on the wrist action shaker for 5 hours at room temperature.
2. Centrifuge the sample for 30 minutes at 2750 rpm.
3. Decant the supernatant, filter thru a 0.2 μm nylon syringe filter.

4. Add five drops of 1:10 HNO_3 to the sample. Store the sample in the refrigerator until ICP analysis.
5. Wash the residue with 8 mL of deionized water by vigorous hand shaking followed by 30 min in the centrifuge at 2750 rpm.
6. Decant and discard the supernatant. Save the residue for the next extraction step.

Bound-to-Fe & Mn Oxides Fraction

1. Add 20 mL 0.04 M $NH_2OH{\cdot}HCl$ in 25% (v/v) CH_3COOH to the residue collected from the bound-to-carbonate fraction. Extract with occasional hand agitation for 6 hours in a water filled beaker on a hot plate at 96º C.
2. Centrifuge the sample for 30 minutes at 2750 rpm.
3. Decant the supernatant, filter thru a 0.2 μm nylon syringe filter.
4. Add five drops of 1:10 HNO_3 to the sample. Store the sample in the refrigerator until ICP analysis.
5. Wash the residue with 8 mL of deionized water by vigorous hand shaking followed by 30 min in the centrifuge at 2750 rpm.
6. Decant and discard the supernatant. Save the residue for the next extraction step.

Bound-to-Organic Matter Fraction

1. Add 3 mL of 0.02 M HNO_3 and 5 mL of 30% H_2O_2 (adjusted to pH 2 with HNO_3) to the residue collected from the bound-to-Fe & Mn oxide fraction.
2. Heat in a water bath at 85ºC for 2 hours.

3. Add 3 mL of 30% H_2O_2 (adjusted to pH 2 with HNO_3).
4. Heat in a water bath at 85ºC for 3 hours with intermittent agitation.
5. Let cool to room temperature.
6. Add 5 ml of 3.2 M CH_3COONH_4 in 20% (v/v) HNO_3.
7. Dilute to 20 mL with deionized water.
8. Agitate continuously with the wrist action shaker for 30 minutes
7. Centrifuge the sample for 30 minutes at 2750 rpm.
8. Decant the supernatant, filter thru a 0.2 μm nylon syringe filter.
9. Add five drops of 1:10 HNO_3 to the sample. Store the sample in the refrigerator until ICP analysis.

Appendix 2 cont. Chemical reagent protocol.

Magnesium Chloride ($MgCl_2 \cdot 6H_2O$)
Amount needed: 1 L of 1 M $MgCl_2 \cdot 6H_2O$ @ pH 7
Add 203.31 grams of $MgCl_2$ to 1 L of deionized water
Adjust pH with addition of 1:10 NaOH.

Sodium Acetate ($CH_3COOHNa \cdot 3H_2O$)
Amount needed: 1 L of 1 M $CH_3COOHNa \cdot 3H_2O_2O$ @ pH 5
Add 136.08 grams of $CH_3COOHNa \cdot 3H_2O$ to 1 L of deionized water
Adjust pH with addition of CH_3COOH

Hydroxylamine Hydrochloride ($NH_2OH \cdot HCl$)
Amount needed: 1 L of 0.04 M $NH_2OH \cdot HCl$ 25% (v/v) CH_3COOH
Add 2.78 grams of $NH_2OH \cdot HCl$ to mixture of 250 mL CH_3COOH & 750 mL deionized water

Nitric Acid (HNO_3)
Amount needed: 1 L of 0.02 M HNO_3
Add 1.28 mL of 15.6 M HNO_3 to 1 L of deionized water.

Hydrogen Peroxide (H_2O_2)
Amount needed: 500 mL of 30% H_2O_2 @ pH 2
Adjust pH with addition of HNO_3

Ammonium Acetate (CH_3COONH_4)
Amount needed: 1 L of 3.2 M CH_3COONH_4 in 20% (v/v) HNO_3
Add 246.66 grams CH_3COONH_4 to mixture of 200 mL HNO_3 to 800 mL deionized water

Appendix 3. Soil lead concentrations. BDL = Below Detection Limits

		Range		Range		Range		Range	
Soil Fraction	Depth	Sample	Pb Conc. (mg/kg)	Sample	Pb Conc. (mg/kg)	Sample	Pb Conc. (mg/kg)	Sample	Pb Conc. (mg/kg)
Water Soluble	A-Horizon	SR-6-a1	8.96	SR-12-a1	BDL	SR-13-a1	BDL	SR-14-a1	BDL
	A-10 cm	SR-6-a2	0.74	SR-12-a2	0.84	SR-13-a2	BDL	SR-14-a2	0.405
	10-30 cm	SR-6-a3	0.33	SR-12-a3	BDL	SR-13-a3	BDL	SR-14-a3	BDL
	30-50 cm	SR-6-a4	0.56	SR-12-a4	BDL	SR-13-a4	BDL	SR-14-a4	BDL
Exchangeable	A-Horizon	SR-6-b1	100.42	SR-12-b1	0.78	SR-13-b1	4.976	SR-14-b1	0.16
	A-10 cm	SR-6-b2	8.05	SR-12-b2	BDL	SR-13-b2	1.664	SR-14-b2	0.496
	10-30 cm	SR-6-b3	4.85	SR-12-b3	0.34	SR-13-b3	0.328	SR-14-b3	0.08
	30-50 cm	SR-6-b4	4.01	SR-12-b4	BDL	SR-13-b4	1.048	SR-14-b4	0.136
Bound-to-Carbonates	A-Horizon	SR-6-c1	2434.30	SR-12-c1	231.256	SR-13-c1	120.296	SR-14-c1	29.976
	A-10 cm	SR-6-c2	52.70	SR-12-c2	8.84	SR-13-c2	8.944	SR-14-c2	4.36
	10-30 cm	SR-6-c3	5.01	SR-12-c3	6.936	SR-13-c3	6.424	SR-14-c3	4.2
	30-50 cm	SR-6-c4	5.08	SR-12-c4	7.152	SR-13-c4	7.496	SR-14-c4	4.208
Bound-to-Fe & Mn Oxides	A-Horizon	SR-6-d1	1485.80	SR-12-d1	210.8	SR-13-d1	207	SR-14-d1	57
	A-10 cm	SR-6-d2	77.60	SR-12-d2	80.6	SR-13-d2	69.6	SR-14-d2	12.94
	10-30 cm	SR-6-d3	39.00	SR-12-d3	45.8	SR-13-d3	67	SR-14-d3	16.72
	30-50 cm	SR-6-d4	35.40	SR-12-d4	75.8	SR-13-d4	74.4	SR-14-d4	12.78
Bound-to-Organic Matter	A-Horizon	SR-6-e1	1318.26	SR-12-e1	743.26	SR-13-e1	206.46	SR-14-e1	13.68
	A-10 cm	SR-6-e2	7.08	SR-12-e2	12.8	SR-13-e2	5.44	SR-14-e2	3.08
	10-30 cm	SR-6-e3	4.06	SR-12-e3	7.02	SR-13-e3	4.84	SR-14-e3	3.16
	30-50 cm	SR-6-e4	6.62	SR-12-e4	5.1	SR-13-e4	7.5	SR-14-e4	4.06

Appendix 3 cont. Soil lead concentrations. BDL = Below Detection Limits

		Range		Range		Range		Range	
Soil Fraction	Depth	Sample	Pb Conc. (mg/kg)	Sample	Pb Conc. (mg/kg)	Sample	Pb Conc. (mg/kg)	Sample	Pb Conc. (mg/kg)
Water Soluble	A-Horizon	SR-15-a1	.645	SR-16-a1	BDL	SR-17-a1	BDL	SR-18-a1	BDL
	A-10 cm	SR-15-a2	BDL	SR-16-a2	7.71	SR-17-a2	BDL	SR-18-a2	0.405
	10-30 cm	SR-15-a3	BDL	SR-16-a3	BDL	SR-17-a3	BDL	SR-18-a3	BDL
	30-50 cm	SR-15-a4	BDL	SR-16-a4	1.8	SR-17-a4	BDL	SR-18-a4	BDL
Exchangeable	A-Horizon	SR-15-b1	0.68	SR-16-b1	0.32	SR-17-b1	BDL	SR-18-b1	0.16
	A-10 cm	SR-15-b2	0.504	SR-16-b2	1.432	SR-17-b2	BDL	SR-18-b2	0.496
	10-30 cm	SR-15-b3	0.408	SR-16-b3	BDL	SR-17-b3	BDL	SR-18-b3	0.08
	30-50 cm	SR-15-b4	0.496	SR-16-b4	0.624	SR-17-b4	BDL	SR-18-b4	0.136
Bound-to-Carbonates	A-Horizon	SR-15-c1	52.056	SR-16-c1	10.512	SR-17-c1	12.344	SR-18-c1	29.976
	A-10 cm	SR-15-c2	7.496	SR-16-c2	4.296	SR-17-c2	6.616	SR-18-c2	4.36
	10-30 cm	SR-15-c3	6.44	SR-16-c3	4.384	SR-17-c3	6.416	SR-18-c3	4.2
	30-50 cm	SR-15-c4	7.44	SR-16-c4	4.944	SR-17-c4	6.512	SR-18-c4	4.208
Bound-to-Fe & Mn Oxides	A-Horizon	SR-15-d1	175.6	SR-16-d1	42.2	SR-17-d1	87.6	SR-18-d1	57
	A-10 cm	SR-15-d2	59.6	SR-16-d2	15.84	SR-17-d2	67.2	SR-18-d2	12.94
	10-30 cm	SR-15-d3	69.6	SR-16-d3	17.72	SR-17-d3	67.6	SR-18-d3	16.72
	30-50 cm	SR-15-d4	63.6	SR-16-d4	14.16	SR-17-d4	64.6	SR-18-d4	12.78
Bound-to-Organic Matter	A-Horizon	SR-15-e1	6.56	SR-16-e1	6.68	SR-17-e1	9.5	SR-18-e1	13.68
	A-10 cm	SR-15-e2	12	SR-16-e2	2.48	SR-17-e2	12.02	SR-18-e2	3.08
	10-30 cm	SR-15-e3	8.7	SR-16-e3	3.86	SR-17-e3	7.04	SR-18-e3	3.16
	30-50 cm	SR-15-e4	6.76	SR-16-e4	5.12	SR-17-e4	8.14	SR-18-e4	4.06

Appendix 3 cont. Soil lead concentrations. BDL = Below Detection Limits

		Control		Range		Range		Range	
Soil Fraction	Depth	Sample	Pb Conc. (mg/kg)	Sample	Pb Conc. (mg/kg)	Sample	Pb Conc. (mg/kg)	Sample	Pb Conc. (mg/kg)
Water Soluble	A-Horizon	SR-19-a1	BDL	SR-21-a1	0.795	SR-22-a1	0.27	SR-23-a1	15.84
	A-10 cm	SR-19-a2	BDL	SR-21-a2	BDL	SR-22-a2	39	SR-23-a2	0.195
	10-30 cm	SR-19-a3	BDL	SR-21-a3	BDL	SR-22-a3	BDL	SR-23-a3	BDL
	30-50 cm	SR-19-a4	BDL	SR-21-a4	BDL	SR-22-a4	BDL	SR-23-a4	0.345
Exchangeable	A-Horizon	SR-19-b1	BDL	SR-21-b1	7.632	SR-22-b1	149.616	SR-23-b1	254.496
	A-10 cm	SR-19-b2	BDL	SR-21-b2	BDL	SR-22-b2	23.768	SR-23-b2	5.12
	10-30 cm	SR-19-b3	0.104	SR-21-b3	BDL	SR-22-b3	1.656	SR-23-b3	0.616
	30-50 cm	SR-19-b4	0.616	SR-21-b4	BDL	SR-22-b4	4.984	SR-23-b4	0.264
Bound-to-Carbonates	A-Horizon	SR-19-c1	4.776	SR-21-c1	65.416	SR-22-c1	3574.296	SR-23-c1	3375.096
	A-10 cm	SR-19-c2	4.456	SR-21-c2	4.848	SR-22-c2	23.232	SR-23-c2	17.496
	10-30 cm	SR-19-c3	4.776	SR-21-c3	4.416	SR-22-c3	7.272	SR-23-c3	6.256
	30-50 cm	SR-19-c4	5.768	SR-21-c4	4.416	SR-22-c4	17.696	SR-23-c4	4.912
Bound-to-Fe & Mn Oxides	A-Horizon	SR-19-d1	21	SR-21-d1	100.4	SR-22-d1	1755.8	SR-23-d1	2179.8
	A-10 cm	SR-19-d2	18.12	SR-21-d2	23.4	SR-22-d2	46.2	SR-23-d2	45.2
	10-30 cm	SR-19-d3	18.36	SR-21-d3	23.2	SR-22-d3	23.6	SR-23-d3	2.7
	30-50 cm	SR-19-d4	14.96	SR-21-d4	20.6	SR-22-d4	32.6	SR-23-d4	BDL
Bound-to-Organic Matter	A-Horizon	SR-19-e1	0.46	SR-21-e1	11.08	SR-22-e1	1732.26	SR-23-e1	1505.26
	A-10 cm	SR-19-e2	3.56	SR-21-e2	2.88	SR-22-e2	12.2	SR-23-e2	14.52
	10-30 cm	SR-19-e3	1.08	SR-21-e3	2.48	SR-22-e3	5.24	SR-23-e3	0.22
	30-50 cm	SR-19-e4	4.52	SR-21-e4	2.92	SR-22-e4	5.36	SR-23-e4	5.3

Appendix 3 cont. Soil lead concentrations. BDL = Below Detection Limits

		Range		Range		Range		Range	
Soil Fraction	Depth	Sample	Pb Conc. (mg/kg)	Sample	Pb Conc. (mg/kg)	Sample	Pb Conc. (mg/kg)	Sample	Pb Conc. (mg/kg)
Water Soluble	A-Horizon	SR-24-a1	BDL	SR-25-a1	2.91	SR-26-a1	BDL	SR-27-a1	126.855
	A-10 cm	SR-24-a2	BDL	SR-25-a2	BDL	SR-26-a2	BDL	SR-27-a2	1.185
	10-30 cm	SR-24-a3	BDL	SR-25-a3	BDL	SR-26-a3	BDL	SR-27-a3	0.195
	30-50 cm	SR-24-a4	BDL	SR-25-a4	4.695	SR-26-a4	BDL	SR-27-a4	BDL
Exchangeable	A-Horizon	SR-24-b1	10.896	SR-25-b1	83.136	SR-26-b1	72.816	SR-27-b1	26.56
	A-10 cm	SR-24-b2	0.632	SR-25-b2	2.784	SR-26-b2	2.488	SR-27-b2	0.144
	10-30 cm	SR-24-b3	0.304	SR-25-b3	0.32	SR-26-b3	1.072	SR-27-b3	0.224
	30-50 cm	SR-24-b4	0.392	SR-25-b4	4.44	SR-26-b4	1.048	SR-27-b4	0.496
Bound-to-Carbonates	A-Horizon	SR-24-c1	111.976	SR-25-c1	932.696	SR-26-c1	161.736	SR-27-c1	19.08
	A-10 cm	SR-24-c2	7.576	SR-25-c2	17.136	SR-26-c2	8.728	SR-27-c2	4.888
	10-30 cm	SR-24-c3	5.232	SR-25-c3	5.6	SR-26-c3	6.608	SR-27-c3	5.488
	30-50 cm	SR-24-c4	5.296	SR-25-c4	10.184	SR-26-c4	5.8	SR-27-c4	5.336
Bound-to-Fe & Mn Oxides	A-Horizon	SR-24-d1	97.8	SR-25-d1	866.2	SR-26-d1	170.8	SR-27-d1	37.2
	A-10 cm	SR-24-d2	2.88	SR-25-d2	19.24	SR-26-d2	BDL	SR-27-d2	2.86
	10-30 cm	SR-24-d3	BDL	SR-25-d3	BDL	SR-26-d3	BDL	SR-27-d3	BDL
	30-50 cm	SR-24-d4	BDL	SR-25-d4	BDL	SR-26-d4	BDL	SR-27-d4	5.04
Bound-to-Organic Matter	A-Horizon	SR-24-e1	7.4	SR-25-e1	252.26	SR-26-e1	24.02	SR-27-e1	7.74
	A-10 cm	SR-24-e2	0.44	SR-25-e2	9.6	SR-26-e2	5.54	SR-27-e2	3.14
	10-30 cm	SR-24-e3	0.44	SR-25-e3	21.68	SR-26-e3	6.38	SR-27-e3	3.96
	30-50 cm	SR-24-e4	0.4	SR-25-e4	3.88	SR-26-e4	8.46	SR-27-e4	4.54

Appendix 3 cont. Soil lead concentrations. BDL = Below Detection Limits

		Range		Range		Control		Control	
Soil Fraction	Depth	Sample	Pb Conc. (mg/kg)	Sample	Pb Conc. (mg/kg)	Sample	Pb Conc. (mg/kg)	Sample	Pb Conc. (mg/kg)
Water Soluble	A-Horizon	SR-28-a1	11.205	SR-29-a1	0.6	SR-33-a1	BDL	SR-34-a1	1.545
	A-10 cm	SR-28-a2	0.21	SR-29-a2	2.04	SR-33-a2	BDL	SR-34-a2	BDL
	10-30 cm	SR-28-a3	0.225	SR-29-a3	BDL	SR-33-a3	0.885	SR-34-a3	BDL
	30-50 cm	SR-28-a4	0.225	SR-29-a4	1.02	SR-33-a4	BDL	SR-34-a4	BDL
Exchangeable	A-Horizon	SR-28-b1	31.928	SR-29-b1	10.656	SR-33-b1	0.072	SR-34-b1	BDL
	A-10 cm	SR-28-b2	2.96	SR-29-b2	1.512	SR-33-b2	0.424	SR-34-b2	0.2
	10-30 cm	SR-28-b3	0.288	SR-29-b3	0.392	SR-33-b3	0.448	SR-34-b3	0.576
	30-50 cm	SR-28-b4	0.224	SR-29-b4	0.08	SR-33-b4	0.56	SR-34-b4	0.528
Bound-to-Carbonates	A-Horizon	SR-28-c1	34.088	SR-29-c1	87.736	SR-33-c1	4.8	SR-34-c1	4.736
	A-10 cm	SR-28-c2	5.176	SR-29-c2	6.016	SR-33-c2	4.616	SR-34-c2	5.536
	10-30 cm	SR-28-c3	4.848	SR-29-c3	5	SR-33-c3	4.824	SR-34-c3	5.784
	30-50 cm	SR-28-c4	4.968	SR-29-c4	4.36	SR-33-c4	5.576	SR-34-c4	5.888
Bound-to-Fe & Mn Oxides	A-Horizon	SR-28-d1	61	SR-29-d1	62.8	SR-33-d1	7	SR-34-d1	10.6
	A-10 cm	SR-28-d2	BDL	SR-29-d2	1.74	SR-33-d2	10.8	SR-34-d2	12
	10-30 cm	SR-28-d3	BDL	SR-29-d3	BDL	SR-33-d3	12.2	SR-34-d3	9.4
	30-50 cm	SR-28-d4	BDL	SR-29-d4	1.9	SR-33-d4	13.2	SR-34-d4	9.6
Bound-to-Organic Matter	A-Horizon	SR-28-e1	15.26	SR-29-e1	9.78	SR-33-e1	1.06	SR-34-e1	1.66
	A-10 cm	SR-28-e2	2.78	SR-29-e2	3.62	SR-33-e2	2.32	SR-34-e2	3.38
	10-30 cm	SR-28-e3	5.9	SR-29-e3	4.78	SR-33-e3	4.34	SR-34-e3	4.14
	30-50 cm	SR-28-e4	5.82	SR-29-e4	2.84	SR-33-e4	4.06	SR-34-e4	3.22

Appendix 3 cont. Soil lead concentrations. BDL = Below Detection Limits

		Control		Control	
Soil Fraction	Depth	Sample	Pb Conc. (mg/kg)	Sample	Pb Conc. (mg/kg)
Water Soluble	A-Horizon	SR-35-a1	0.315	SR-36-a1	BDL
	A-10 cm	SR-35-a2	BDL	SR-36-a2	BDL
	10-30 cm	SR-35-a3	BDL	SR-36-a3	BDL
	30-50 cm	SR-35-a4	BDL	SR-36-a4	BDL
Exchangeable	A-Horizon	SR-35-b1	BDL	SR-36-b1	BDL
	A-10 cm	SR-35-b2	0.312	SR-36-b2	0.168
	10-30 cm	SR-35-b3	0.264	SR-36-b3	BDL
	30-50 cm	SR-35-b4	0.328	SR-36-b4	BDL
Bound-to-Carbonates	A-Horizon	SR-35-c1	4.168	SR-36-c1	4.136
	A-10 cm	SR-35-c2	5.128	SR-36-c2	5.232
	10-30 cm	SR-35-c3	5.152	SR-36-c3	4.552
	30-50 cm	SR-35-c4	4.976	SR-36-c4	4.008
Bound-to-Fe & Mn Oxides	A-Horizon	SR-35-d1	0.4	SR-36-d1	7.6
	A-10 cm	SR-35-d2	BDL	SR-36-d2	23
	10-30 cm	SR-35-d3	8.2	SR-36-d3	7.4
	30-50 cm	SR-35-d4	6.6	SR-36-d4	0.8
Bound-to-Organic Matter	A-Horizon	SR-35-e1	2.86	SR-36-e1	1.88
	A-10 cm	SR-35-e2	2.94	SR-36-e2	1.78
	10-30 cm	SR-35-e3	3.7	SR-36-e3	1.3
	30-50 cm	SR-35-e4	3.02	SR-36-e4	0.56

Appendix 4. Gibbs free energies of formation at 298.15°K and 1 atm from (Schock 1996).

Species	Mineral	ΔG_f^0 kJ/mol
Pb		0.0
Pb^{2+}		-24.39
$PbOH^+$		-220.33
$Pb(OH)_2^0$		-402.12
$Pb(OH)_3^-$		-575.72
$Pb(OH)_4^{2-}$		-746.43
PbO	Massicot	-188.61
PbO	Litharge	-189.66
PbO_2	Plattnerite	-217.48
Pb_3O_4	Minium	-622.16
$PbCO_3$	Cerussite	-625.51
$Pb_3(CO_3)_2(OH)_2$	Hydrocerussite	-1710.84
H_2O		-237.19
$H_2CO_3^0$		-623.21
HCO_3^-		-586.93
CO_3^{2-}		-527.98

Appendix 5. Soil pH's for shotgun range and background samples.

(* denotes background sample)

Sample	Depth	pH
SR-6	A-Horizon	8.20
	A-10 cm	7.22
	10-30 cm	6.39
	30-50 cm	4.79
SR-12	A horizon	7.28
	A - 10 cm	6.19
	10 - 30 cm	4.73
	30 - 50 cm	4.58
SR-13	A horizon	6.95
	A - 10 cm	5.69
	10 - 30 cm	4.69
	30 - 50 cm	4.49
SR-14	A horizon	7.21
	A - 10 cm	5.78
	10 - 30 cm	4.83
	30 - 50 cm	4.58
SR-15	A horizon	6.77
	A - 10 cm	5.27
	10 - 30 cm	4.62
	30 - 50 cm	4.38
SR-16	A horizon	7.28
	A - 10 cm	6.61
	10 - 30 cm	5.77
	30 - 50 cm	4.83

Sample	Depth	pH
SR-17	A horizon	6.76
	A - 10 cm	5.55
	10 - 30 cm	4.47
	30 - 50 cm	4.30
SR-18	A horizon	6.20
	A - 10 cm	5.72
	10 - 30 cm	4.67
	30 - 50 cm	4.39
SR-19*	A horizon	5.63
	A - 10 cm	5.31
	10 - 30 cm	4.52
	30 - 50 cm	4.32
SR-21	A horizon	6.51
	A - 10 cm	5.39
	10 - 30 cm	4.87
	30 - 50 cm	4.81
SR-22	A horizon	7.22
	A - 10 cm	4.81
	10 - 30 cm	4.74
	30 - 50 cm	4.69
SR-23	A horizon	6.35
	A - 10 cm	5.15
	10 - 30 cm	4.83
	30 - 50 cm	4.66

Appendix 5 cont. Soil pH's for shotgun range and background samples.
(* denotes background sample)

Sample	Depth	pH
SR-24	A horizon	6.27
	A - 10 cm	5.19
	10 - 30 cm	4.62
	30 - 50 cm	4.55
SR-25	A horizon	6.32
	A - 10 cm	5.29
	10 - 30 cm	4.45
	30 - 50 cm	4.76
SR-26	A horizon	5.21
	A - 10 cm	4.38
	10 - 30 cm	4.31
	30 - 50 cm	4.33
SR-27	A horizon	4.80
	A - 10 cm	4.48
	10 - 30 cm	4.51
	30 - 50 cm	4.13
SR-28	A horizon	6.27
	A - 10 cm	4.66
	10 - 30 cm	4.30
	30 - 50 cm	4.52

Sample	Depth	pH
SR-29	A horizon	7.31
	A - 10 cm	5.15
	10 - 30 cm	4.47
	30 - 50 cm	4.45
SR-33*	A horizon	5.59
	A - 10 cm	4.83
	10 - 30 cm	4.67
	30 - 50 cm	5.09
SR-34*	A horizon	6.03
	A - 10 cm	5.72
	10 - 30 cm	4.78
	30 - 50 cm	4.67
SR-35*	A horizon	5.74
	A - 10 cm	4.57
	10 - 30 cm	4.89
	30 - 50 cm	5.01
SR-36*	A horizon	5.89
	A - 10 cm	5.59
	10 - 30 cm	5.14
	30 - 50 cm	4.47

Appendix 6. Total lead concentrations of the soil A-horizon.
(* denotes background sample)

Sample	ppm Pb
SR-6	37980
SR-12	2570
SR-13	2140
SR-14	849
SR-15	1020
SR-16	640
SR-17	1240
SR-18	1130
SR-19*	362
SR-21	3460
SR-22	30420
SR-23	19190
SR-24	4520
SR-25	12100
SR-26	4130
SR-27	5070
SR-28	3270
SR-29	8870
SR-33*	324
SR-34*	178
SR-35*	98
SR-36*	327